

# A new approach to real time optimization of the Tennessee Eastman challenge problem

M. Golshan, R. Bozorgmehry boozarjomehry\*, M.R. Pishvaie

*Department of Chemical and Petroleum Engineering, Sharif University of Technology, Tehran, Iran*

Received 28 November 2004; received in revised form 11 June 2005; accepted 14 June 2005

---

## Abstract

On-line optimization for the base case of the Tennessee Eastman (TE) challenge problem is presented; furthermore, an interesting operating condition near base case has been obtained, which results in a lower cost function. The proposed method is based on the estimation of the internal states and the time varying parameters of the process model based on an Extended Kalman filter. The sequential quadratic programming method has been used to accomplish the non-linear programming (NLP) task. The objective function is the operational cost while the constraints are the reactor mass balance, safe operation of the process equipment, and the conditions that satisfy the product quality and flow. The optimizer is triggered every 8 h, and determines an optimal set of process operating conditions. Note, the calculations are completed in some 5–15 s by an Intell PIII 800 MHz with 256 MB of RAM. The study shows that the proposed algorithm outperforms the alternative algorithms developed by other researchers both in speed and results.

© 2005 Published by Elsevier B.V.

*Keywords:* Tennessee Eastman; Real time optimization; Supervisory control; Extended Kalman filter

---

## 1. Introduction

Real time optimization (RTO) methods have been recently welcome by both industry and academia [1–4]. This is due to the following facts:

1. Tougher competition in the volatile market necessitates minimization of the production cost.
2. The cost of computational resources both for hardware and software is getting lower and lower.
3. Environmental regulations are getting more difficult to meet.

In order to show the efficient performance of the RTO algorithm, they should be used in the optimization of a benchmark process representing most of the challenges exist in industrial plants. Tennessee Eastman (TE) process is a challenging benchmark for plant-wide control and optimization that has been proposed by Downs and Vogel [5]. One of the

main characteristics for this process is the fact that it is open loop unstable and gets shutdown within an hour if it operates in an open loop manner.

In this paper a new approach in the real time optimization of the TE process that leads to the minimum achievable production cost is proposed. The minimum achievable production cost obtained by Ricker in an offline manner [6]. At first the plant characteristics are described and then appropriate control structure to stabilize the process is explained. In the third section a non-linear model for the process used for the optimization purposes is introduced. Detail structure and constituting elements of the real time optimizer are presented in Section 4. The last section contains the results obtained by the proposed algorithm and the comparison of these results with those obtained by other researchers.

## 2. Process description

Tennessee Eastman challenge process, involves five major units including a two-phase reactor, a partial condenser, a separator, a stripper, and a compressor. The schematic flow

---

\* Corresponding author. Tel.: +98 21 6165403; fax: +98 21 6022853.  
*E-mail address:* brbozorg@sharif.edu (R.B. boozarjomehry).

### Nomenclature

$C_{i,cst}$	cost of component $i$ (\$/kg mol)
$C_{tot}$	hourly production cost (\$/h)
$F_i$	molar flow rate of stream $i$ , (kmol/h)
$F_i^*$	molar “pseudo-feed” of component $i$ (kmol/h), where $i = A, B, \dots, H$ . Added at the feed mixing point
$F_{steam}$	total flow rate of steam used in the plant (kg/h)
$F_{10}^P$	apparent stream 10 flow rate (kmol/h), as indicated by the valve position
$F_{10}^*$	bias adjustment for stream 10 (kmol/h)
$N_{i,m}$	total molar holdup of component $i$ in the feed mixing zone (kmol/h)
$N_{i,p}$	total molar holdup of component $i$ in the stripper bottom product
$N_{i,r}$	total molar holdup of component $i$ in the reactor (kmol/h)
$N_{i,s}$	total molar holdup of component $i$ in the separator (kmol/h)
$P_i^{sat}(T_r)$	vapor pressure of pure $i$ at the reactor temperature
$P_i^{sat}(T_s)$	vapor pressure of pure $i$ at the separator temperature
$P_{i,r}$	partial pressure of $i$ in reactor (kPa)
$P_{i,s}$	partial pressure of $i$ in separator (kPa)
$P_m$	total pressure in the feed mixing zone (and stripper) (kPa)
$P_r$	total pressure in the reactor (kPa)
$P_s$	total pressure in the separator (kPa)
$R_j$	molar rate of reaction $j$ (kmol/h)
$R$	gas constant (1.987 cal/gmol K in equations 22-4 to 24-4 otherwise 8.314 kJ/lmol k)
$t$	time (h)
$T_m$	absolute temperature in the feed mixing zone (359.3 K), assumed constant
$T_r$	absolute temperature in the reactor (K)
$T_s$	absolute temperature in the separator (K)
$V_{Lp}$	liquid volume in the stripper (m <sup>3</sup> )
$V_{Lr}$	liquid volume in the reactor (m <sup>3</sup> )
$V_{Ls}$	liquid volume in the separator (m <sup>3</sup> )
$V_m$	total volume of feed mixing zone (150 m <sup>3</sup> ), assumed constant
$V_r$	total reactor volume (36.8 m <sup>3</sup> ), assumed constant
$V_s$	total separator volume (99.1 m <sup>3</sup> ), assumed constant
$V_{vr}$	vapor volume in the reactor (m <sup>3</sup> )
$V_{vs}$	vapor volume in the separator (m <sup>3</sup> )
$W_{comp}$	compressor power (kW)
$x_{i,j}$	mole fraction of component $i$ in liquid stream $j$
$x_{i,r}$	mole fraction of component $i$ in the reactor liquid

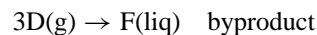
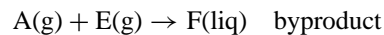
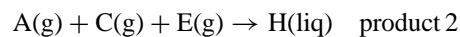
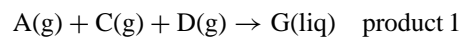
$y_i$	$i$ th element of the output vector, $y$
$y_{i,j}$	mole fraction of component $i$ in vapor stream $j$
$z_{i,j}$	mole fraction of component $i$ in feed stream $j$

### Greek letters

$\alpha_i$	adjustable parameter used in reaction rate equations with nominal value of unity
$\beta_i$	used to adjust flow/pressure drop relation with nominal values of unity
$\gamma_{ir}$	activity coefficient of $i$ in the reactor liquid phase
$\gamma_{is}$	activity coefficient of $i$ in the separator liquid phase
$\nu_{ij}$	stoichiometric coefficient of component $i$ in reaction $j$ , where $i = A, B, \dots, H, j = 1, 2, 3$
$\rho_i$	molar density of pure liquid $i$ (mol/m <sup>3</sup> )
$\phi_i$	stripping factor for component $i$ which is assumed constant
$\chi_{GH}$	purity of G + H in the product (as a fraction)

diagram and instrumentation of this process is shown in Fig. 1 [5].

TE process produces two products from four reactants. Also there is an inert, B, and a byproduct, F, making a total of eight components: A, B, C, D, E, F, G, and H. The following four irreversible and exothermic reactions are taking place in the liquid phase of a two-phase reactor in the presence of a nonvolatile catalyst dissolved in the liquid phase:



Due to the medium volatility of the products, they are getting out of the reactor along the un-reacted gases. The effluent of the reactor passes through a partial condenser whose outlet, which is a two-phase stream, is separated into a gas and a liquid streams in the flash separator. The overhead of the separator is pressurized and recycled to the reactor. The liquid stream getting out of the separator is sent to a stripper in which the reactants ‘D’ and ‘E’ are stripped out of the liquid phase and sent back to the reactor. The bottom product of the stripper mainly consists of ‘G’ and ‘H’ is the main product of the plant. Due to the presence of a non-condensable component (‘B’ which is an inert component) in one of the inlet streams (stream 4) and to avoid the build up of excess reactants and the byproduct ‘F’, a purge stream (stream 9) is used.

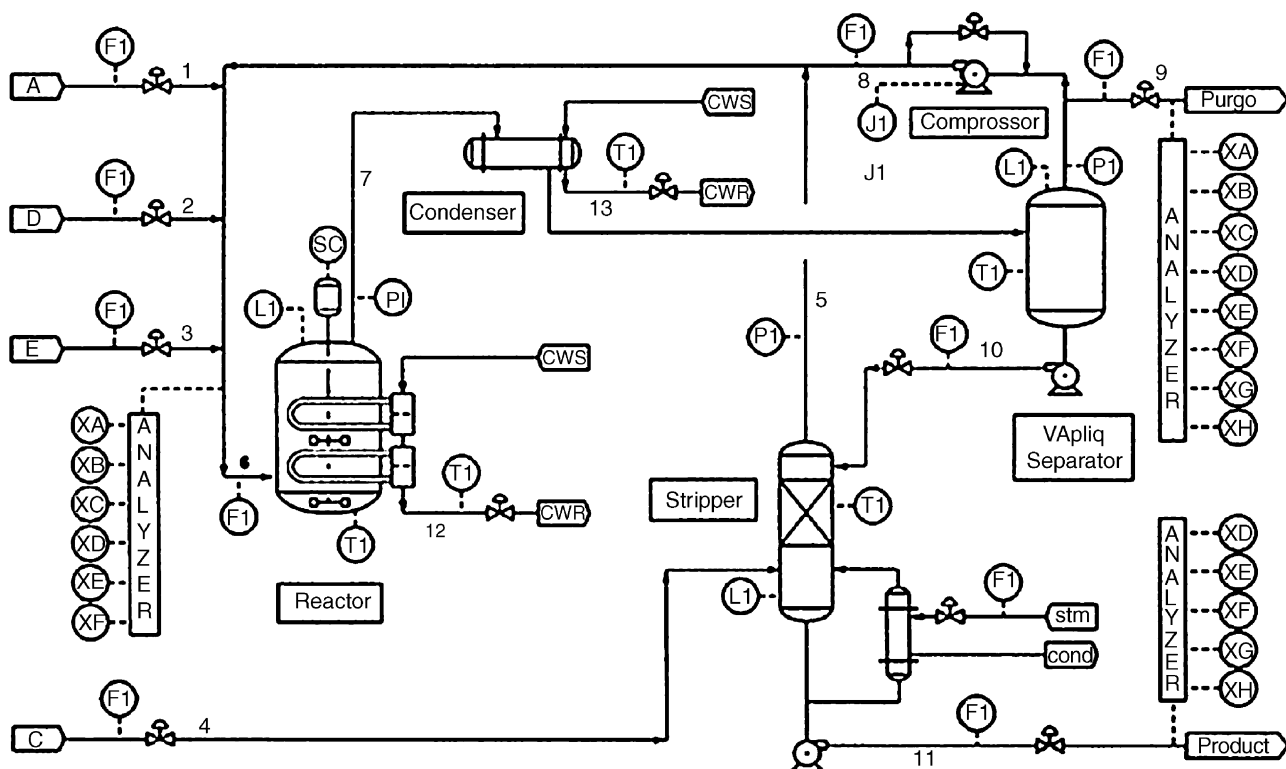


Fig. 1. Schematic diagram of Tennessee Eastman process.

Downs and Vogel developed and offered a Fortran program simulating the dynamic behavior of the process for various conditions, and asked the research community to deal with this simulator as a black box and not to change the code. They provided 41 measurements and 12 manipulating variables for the process in their code. The measurements have been corrupted by zero mean white noises. Tables 1a and 1b represent the measurements and manipulating variables.

### 3. Process control strategy

The primary control objective for the TE process is to maintain a specified ratio of G/H in the product and to maintain the specified production rate during normal process operating conditions and during process upsets. Note that the four feed streams are products of other upstream facilities in the industrial complex and distillation processes are fed by the product stream to get separated into products G and H. Hence, the control structure should enforce the constraints on variation frequency of product flow. Furthermore, it should enforce the constraints corresponding to safe process operation to avoid process shutdown.

In this work the control structure proposed by McAvoy and Ye [7] is used for process control and stabilization. The simulation studies have shown that this control strategy is appropriate for the RTO system proposed in this paper. This control structure consists of 10 cascade loops and 2 single loops. The control configurations as well as tunings are shown in Table 2.

### 4. Real time optimization (RTO)

In order for chemical plants to survive in the volatile and highly competitive market, they are getting more and more integrated. The integration of the process improves overall economics of the plant. However, it makes it harder to control. The plant can no longer be controlled at the unit operation level and achieving the control objectives requires considering the operation of the whole plant. Real time optimization takes these ideas one step further with the addition of an economic objective which should be taken into account while the plant is controlled. In order for the plant to work at the optimum condition, the optimum values for the controllers' set points have to be found by the RTO.

The RTO algorithm proposed in this work consists of the simulator of the TE process which is the Fortran code proposed by Downs and Vogel imported in MATLAB, the state space model of the TE process proposed by Ricker and Lee [8], an extended Kalman filter (EKF) used to update the available parameters in Ricker's model [8] and the optimization algorithm which is based on sequential quadratic programming (SQP) method. The arrangement of these constituting elements and the flow of information among them are shown in Fig. 2. These elements are described in next subsections.

#### 4.1. TE process model

Ricker obtained a dynamic model which only covers the material balance of the process. This model is presented in

Table 1a  
Available measured variables in TE Plant

Variable number	Variable name
1	A feed (stream 1)
2	D feed (stream 2)
3	E feed (stream 3)
4	A and C feed (stream 4)
5	Recycle flow (stream 8)
6	Reactor feed rate (stream 6)
7	Reactor pressure
8	Reactor level
9	Reactor temperature
10	Purge rate (stream 9)
11	Product separator temperature
12	Product separator level
13	Product separator pressure
14	Product separator underflow (stream 10)
15	Stripper level
16	Stripper pressure
17	Stripper underflow (stream 11)
18	Stripper temperature
19	Stripper steam flow
20	Compressor work
21	Reactor cooling water outlet temperature
22	Separator cooling water outlet temperature
23	Component A in stream 6
24	Component B in stream 6
25	Component C in stream 6
26	Component D in stream 6
27	Component E in stream 6
28	Component F in stream 6
29	Component A in stream 9
30	Component B in stream 9
31	Component C in stream 9
32	Component D in stream 9
33	Component E in stream 9
34	Component F in stream 9
35	Component G in stream 9
36	Component H in stream 9
37	Component D in stream 11
38	Component E in stream 11
39	Component F in stream 11
40	Component G in stream 11
41	Component H in stream 11

Table 1b  
Available manipulating variables in TE plant

Variable number	Variable name
1	D feed flow (stream 2)
2	E feed flow (stream 3)
3	A feed flow (stream 1)
4	A and C feed flow (stream 4)
5	Compressor recycle valve
6	Purge valve (stream 9)
7	Separator pot liquid flow (stream 10)
8	Stripper liquid product flow (stream 11)
9	Stripper steam valve
10	Reactor cooling water flow
11	Condenser cooling water flow
12	Agitator speed

Appendix A and can be shown in the following general form:

$$\dot{x} = f(x, u, d), \quad y = g(x, u, d) \quad (1)$$

Where  $x, u, d$ , are state, input and model parameters, respectively. This model consists of 26 states, 10 inputs, and 15 parameters.

#### 4.2. Parameter updating method

Eqs. (A.1)–(A.23) shows the model used to represent the dynamic behavior of the TE process. This model consists of 26 states and 15 parameters that should be adjusted to eliminate errors in its results. Since all the measurements of the TE process are corrupted by noise, the Extended Kalman Filter seems to be an accurate and efficient estimation method. In fact, using the EKF both the parameters and states of the model can be estimated in an optimal manner [8,9]. In order to estimate the states and model parameters, 16 measurements have been used as the outputs of the process in the EKF.

A general and brief overview of the implemented EKF is presented here for the sake of clarity. Interested readers are referred to the additional literature for further discussion [8–10].

EKF is an optimal observer used for non-linear systems. The optimal gain used in the EKF is the pivot element of the Kalman filter (and other conventional closed-loop observers) is obtained through the minimization of the norm of the difference between the estimated and measured outputs. In general for a non-linear system whose state-space model is defined by Eq. (2):

$$\dot{x} = f(x, u, d) + w^x, \quad \dot{d} = w^d, \quad y = g(x, u, d) + v \quad (2)$$

Assuming that Eq. (3) represents the discrete-time model of the system:

$$\begin{bmatrix} x_{k|k-1} \\ d_{k|k-1} \end{bmatrix} = \begin{bmatrix} Fts(x_{k|k-1}, u_{k-1}, d_{k-1|k-1}) \\ d_{k-1|k-1} \end{bmatrix} \quad (3)$$

the equations corresponding to discrete EKF of the system can be represented by Eq. (4):

$$\begin{bmatrix} x_{k|k} \\ d_{k|k} \end{bmatrix} = \begin{bmatrix} x_{k|k-1} \\ d_{k|k-1} \end{bmatrix} + L_k(y_k - g(x_{k|k-1}, u_{k-1}, d_{k-1|k-1})) \quad (4)$$

Note that the additional term (output injection) is a measurement correction used to establish the parametric closed-loop behavior.

Having estimated the states and parameters of the model, one could easily obtain the estimated output by Eq. (5):

$$y_{k|k} = g(x_{k|k}, u_k, d_{k|k}) \quad (5)$$

In order to minimize the errors in the estimated states and parameters the optimal gain matrix,  $L_k$ , must be calculated as

Table 2  
PI Controllers configuration and tunings of the 12 control loops whose set point used in the RTO

Controlled variables	Manipulated variables	$K_c$	$\tau_i$ (min)
Reactor level	E-feed flow set point	500 (kg/h/%)	200
Stripper level	Product flow set point	-0.5 (m <sup>3</sup> /h/%)	300
Separator level	Its bottom flow set point	-2.5 (m <sup>3</sup> /h/%)	200
Product rate	C-feed flow set point	0.08 (kscmh/m <sup>3</sup> /h)	40
Product G/H ratio	D/E feed ratio	0.05	40
Reactor pressure	A-feed flow set point	-0.0032 (kscmh/kPa)	300
Reactor temperature	Reactor cooling set point	1.0	50
Stripper temperature	Steam flow set point	10.0 (kg/h/°C)	10
Compressor power	Recycle valve	0.08 (%/kW)	20
Mole fraction of B in purge	Purge rate	-0.03 (kscmh/%)	100
Compressor outlet Flow	Condenser cooling set point	1.5 (°C/kscmh)	50
Mole fraction of E in product	Stripper temperature set point	-0.5 (°C/%)	100

follows [8]:

$$L_k = \Sigma_{k|k-1} \Xi_k^T (\Xi_{k|k-1}^T \Sigma_{k|k-1} \Xi_k^T + R^v)^{-1},$$

$$\Sigma_{k|k-1} = \Phi_{k-1} \Sigma_{k-1|k-1} \Phi_{k-1}^T + R^w,$$

$$\Sigma_{k|k} = (I - L_k \Xi_k) \Sigma_{k|k-1} \quad (6)$$

Where  $R^w$  is the covariance of the measurement noise (i.e.,  $R^w = cov\{w^x, w^d\}$ )

$$\Phi = \begin{bmatrix} A_k & B_k \\ 0 & I \end{bmatrix}, \quad \Xi_k = [C_k \quad C_k^d]$$

and  $A_k, B_k^d, C_k,$  and  $C_k^d$  are determined through the following linearization/discretization relations, described in detail by

Lee and Ricker [10]:

$$A_k = \exp(\tilde{A}_k t_s), \quad \tilde{A}_k = \frac{\partial f(x, u, d)}{\partial x} \Big|_{(x=x_{k|k}, u=u_k, d=c^w x_{k|k}^w)},$$

$$B_k^d = \int_0^{t_s} \exp(\tilde{A}_k \tau) d\tau \tilde{B}_k^d,$$

$$\tilde{B}_k^d = \frac{\partial f(x, u, d)}{\partial x} \Big|_{(x=x_{k|k}, u=u_k, d=c^w x_{k|k}^w)},$$

$$C_k = \frac{\partial g(x, d)}{\partial x} \Big|_{(x=x_{k|k-1}, d=c^w x_{k|k-1}^w)},$$

$$C_k^d = \frac{\partial g(x, d)}{\partial x} \Big|_{(x=x_{k|k-1}, d=c^w x_{k|k-1}^w)} \quad (7)$$

To use the above equations one must first initialize the covariance matrices,  $R^w$  and  $R^v$ , and the initial state covariance,  $\Sigma_0|0$ , then the solution is straightforward.

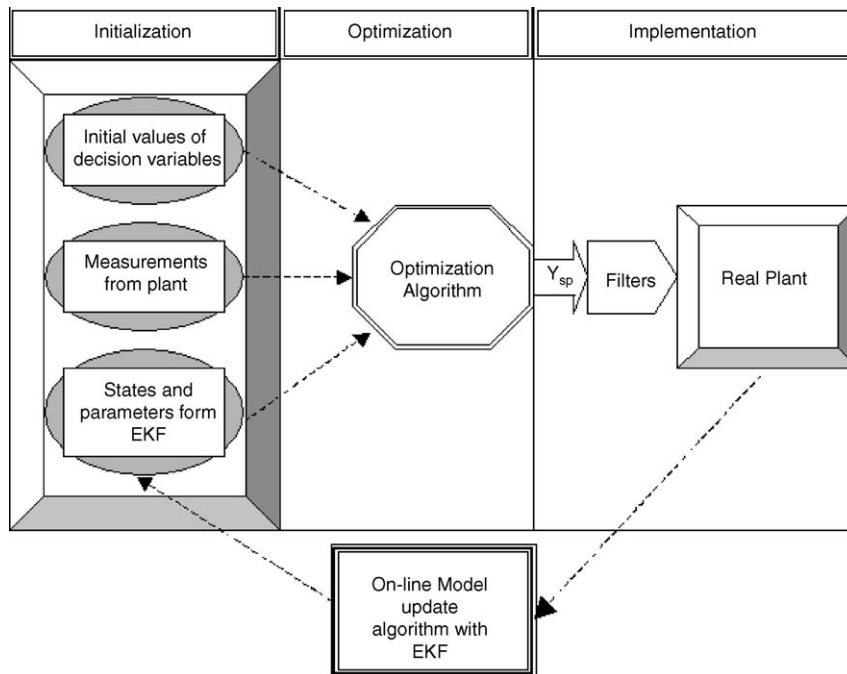


Fig. 2. (a) Schematic diagram of the RTO algorithm and its constituting elements.

### 4.3. Optimization problem

In general each optimization problem can be presented in the following mathematical form:

Optimize  $\Gamma(\mathbf{X}, \mathbf{P})$   
Subject to:

$$\begin{aligned} g_j(\mathbf{X}) &\leq 0 & j = 1, 2, \dots, m \\ l_i(\mathbf{X}) &= 0 & i = 1, 2, \dots, p \end{aligned} \quad (8)$$

where  $\Gamma$  is the objective function,  $\mathbf{P}$  the vector containing various system parameters,  $\mathbf{X}$  the vector containing all decision variables whose optimum values are to be obtained.  $g_j$ ,  $l_i$ , are inequality and equality constraints, respectively. This section represents these parts for the RTO of the TE plant.

#### 4.3.1. Objective function

The objective function used in this work is the hourly operating cost ( $C_{\text{tot}}$ ) in \$/h and should be minimized. It contains the reactant and product losses in the purge and product streams, steam cost and compressor power cost and is calculated by Eq. (9):

$$\begin{aligned} C_{\text{tot}} = & F_9 \sum_{i=A, i \neq B}^H C_{i,\text{cst}} X_{i,9} + F_{11} \sum_{i=D}^F C_{i,\text{cst}} X_{i,11} \\ & + 0.0536 W_{\text{cmp}} + 0.0318 F_{\text{steam}} \end{aligned} \quad (9)$$

The cost of each component,  $C_{i,\text{cst}}$ , in \$/kg mol was provided by Downs and Vogel [5];  $W_{\text{cmp}}$  and  $F_{\text{steam}}$  are compressor power and steam flow rate respectively;  $F_9$ ,  $X_{i,9}$  and  $F_{11}$ ,  $X_{i,11}$  molar flow rate and mole fraction of component 'i' in streams 9 and 11, respectively.

#### 4.3.2. Decision variables

In the McAvoy control strategy for TE there are 10 cascade control loops and two single loop controllers [11]. Hence, this control structure results in 12 set points that can be used as decision variables. However, since one of these set points corresponds to product composition and should be kept constant, this variable cannot be used as the decision variable. Furthermore, the stripper temperature set point has not been used as decision variable either. This is due to the fact that Ricker's model does not contain energy balance of the plant and hence the stripper temperature does not influence it explicitly. The remaining 10 set points are used as the set of decision variables in the real time optimization.

#### 4.3.3. Problem constraints

The objective function should be minimized subject to various constraints. Most of these constraints are non-linear; for instance material balance of various components around the reactor should be satisfied in order to keep the optimization result in the desired range of product quality. However, since the increase in number of constraints makes the optimization

more difficult and lowers the efficiency of the algorithm, one should have a parsimonious approach in the selection of optimization constraints. After thorough studies on the effect of component material balances around the reactor as the optimization constraints, we found out that using the material balance of component 'F' have almost the same effect that selection of all material balances as the constraints do. Hence instead of using all material balances around the reactor as the optimization constraints, material balance of component 'F' around the reactor has been used. It should be noted that although various components have been tested as the basis for this constraint, component 'F' led to best performance of the optimization algorithm. Optimization result must assure the safe operating condition to prevent equipment failure of process shutdown. In order to achieve this, one should consider some additional constraints among which are compressor power and mole fraction of 'E' in the product. However, Ricker's model does not take into account the effect of these two parameters and they are among the decision variables and have an increasing effect on the objective function. Therefore, the optimizer directs them to their corresponding minimum values. On the other hand, setting the compressor work and

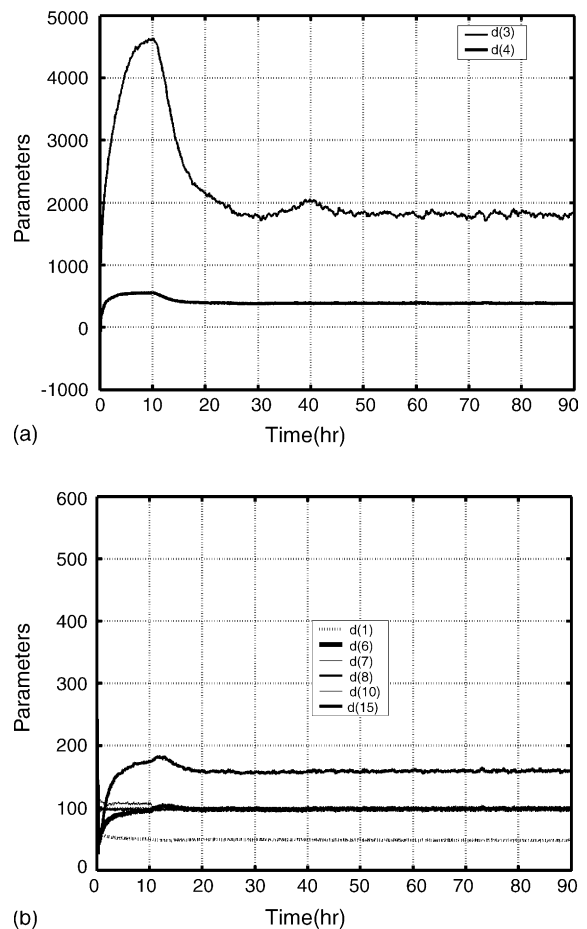


Fig. 3. (a) The reaction rates adjustable parameters d(3), d(4). (b) Some other parameters d(1), d(6), d(7), d(8), d(10), d(15).



mole fraction of ‘E’ in the product to their minimum values would lead to process instability and shutdown. In order to avoid such a situation the minimum of these variables are set to the values around those reported by Ricker [6]. Note the minimum values used for these two constraints do not significantly affect the objective function. For example, changing their values from those reported in the base case to the values obtained at the optimum point would result in only 1.9 \$/h (about 1%) decrease of the cost function.

#### 4.4. Optimization algorithm

Fig. 2 shows the algorithm used to solve the RTO problem. In order for the optimizer to start, the EKF should converge. After the convergence of the EKF, the steady state model obtained from Ricker’s model along with the parameters obtained by EKF and process measurements are used by the optimization algorithm to obtain the optimal set points. The optimization method is based on sequential quadratic programming. Once the optimizer obtained the optimum values

of controllers’ set points these values are introduced to their corresponding controllers through a set of filters whose tasks are to change the controllers’ set points gradually. This is due to the fact that rapid change of controllers’ set points might lead to process instability and shutdown [2]. These filters are all first order linear filters whose time constants have been set to 7 h. Furthermore, since the agitator speed does not take a part in process model and objective function, it has been set to its maximum value due to the fact that it has a positive effect on the rate of reactions.

The efficiency of the RTO algorithm severely depends on the validity of the process states and model parameters obtained from EKF. Fig. 3 shows the performance of the model for some of the estimated parameters and outputs. The parameters whose trends are not shown here does not significantly affect the accuracy of the process model [12,13].

Fig. 4 shows the states of the process model track their corresponding values presented by Ricker [8] perfectly.

Fig. 5 compares some of the estimated output against their corresponding measured values. This figure shows that there is negligible difference between estimated outputs and

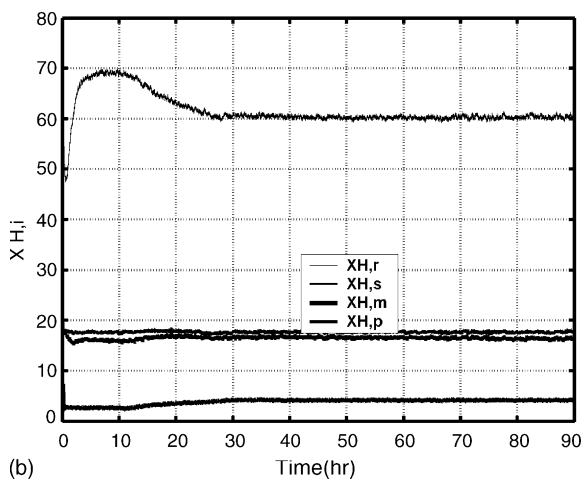
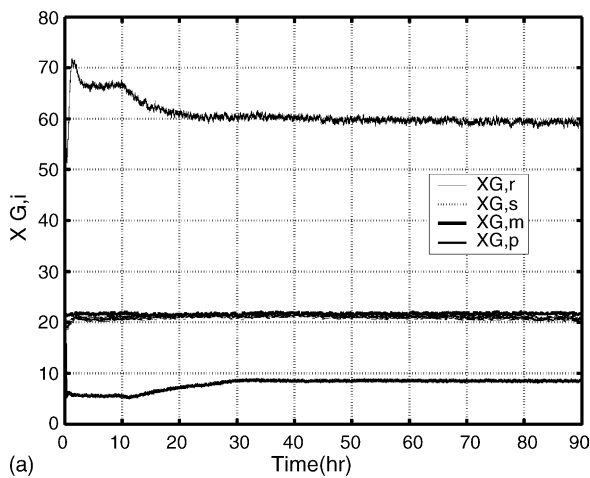


Fig. 4. (a) Moles G in the reactor, separator, mixing zone and stripper; the horizontal lines are those reported by Ricker, (b) as case (a) but for component H.

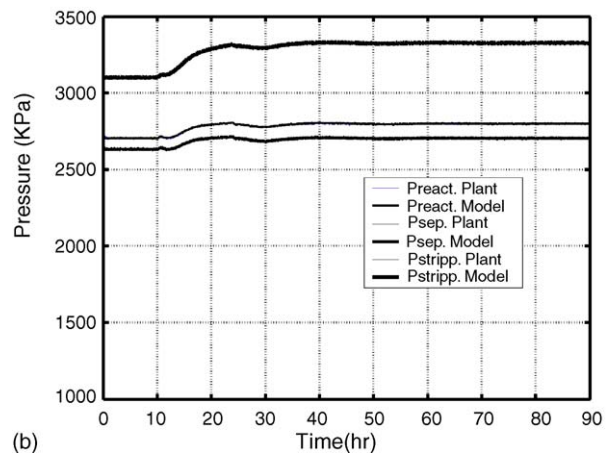
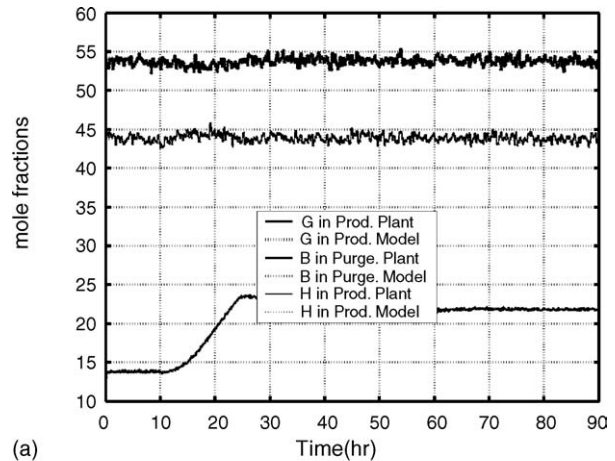


Fig. 5. (a) Comparison of B in purge, G in product, and H in product between model and plant outputs. (b) Comparison of pressures in the reactor, separator, and stripper between model and plant outputs.

measured outputs, which is not detectable even during transient condition.

## 5. Results and discussion

The proposed RTO algorithm has been used to optimize the operation of TE plant working in base case based on two different scenarios. In the first scenario the product flow is fixed to the value given by Downs and Vogel for the base case operation, whereas in the second scenario the product flow rate is maintained near the base case value.

### 5.1. RTO for fixed product flow

In this scenario a constraint corresponding to fixed product flow is among the optimization constraints. The optimizer has been activated every 8 h and determines the optimum operating condition. Fig. 6 shows the trend of cost function during the online optimization. Production cost corresponding to the obtained optimum condition at the steady state is 114 \$/h. Note, according to Fig. 6 the production cost gets to values even less than 114 \$/h, however, this value is due to change in purge valve position which has a major effect on production cost and cannot last at steady state.

The optimum operating conditions obtained by the proposed algorithm have been compared against the optimum condition obtained by Ricker [6] in Table 3. However, Ricker has used noise-free measurements and the exact process model to solve this optimization problem in an offline manner. He has used 50 decision variables that are states of the exact process model and solved the resulting problem by MINOS 5.1. He has emphasized that this optimum point in which the production cost is 114 \$/h is the global minimum that could be obtained using the perfect model with noise-free measurements and in offline manner. It should also be noted that the optimum conditions obtained by Ricker does not result in product flow of 22.949 exactly, where as the optimum

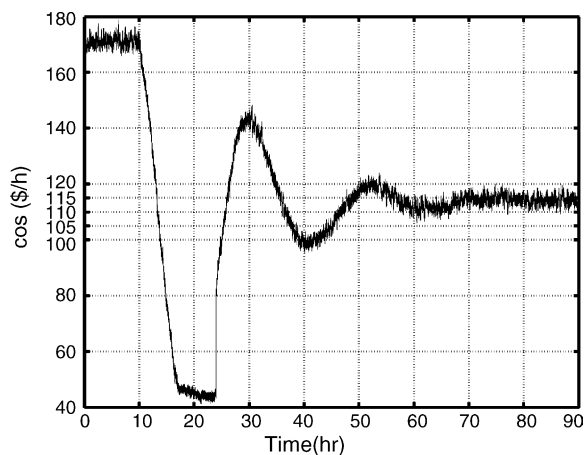


Fig. 6. Cost function during on-line optimization.

Table 3

Comparison of optimization results with base case value and Ricker's results for set points

Decision variable	Base case value	Ricker's results	This paper results
Reactor level (%)	75	65	65
Stripper level (%)	50	50	50
Separator level (%)	50	50	51.9
Product flow (cm/h)	22.949	22.89	22.949
Reactor press (kPa)	2705	2800	2799.9
Reactor temperature (°C)	120.4	122.9	123.3
Compressor work (kW)	341.43	278.9	277
B in purge flow (%)	13.823	21.83	21.8
Recycle flow (kscmh)	26.902	32.18	32.2
E in product (%)	0.83570	0.58	0.56
Cost function	170.6	114.31	114.2

point obtained in this work satisfies this equality constraints exactly.

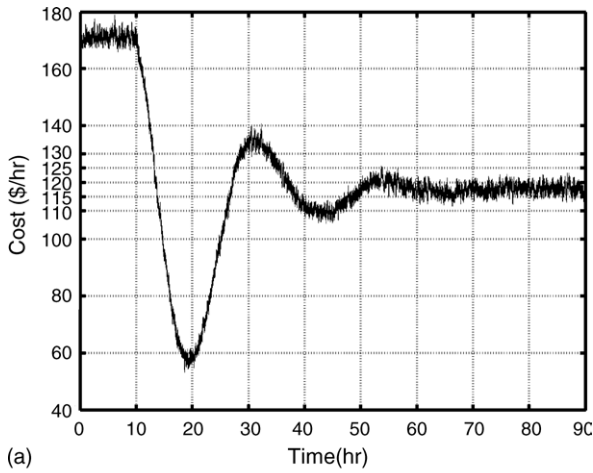
Duval and Riggs [1] has solved the RTO problem of the TE process for the base case based on a steady state model and distributed control configuration proposed by Ricker [11]. However, the optimum point obtained by them would result in the production cost of 120 \$/h. Furthermore, their steady state model consists of 19 decision variables. Despite the fact that optimization method used by Riggs and Duval was similar to the one used in this work, their Real Time Optimizer takes about 5 min to converge, where as the method proposed in this paper takes only 25 s on the similar computer and platform used by Riggs and Duval. This large difference mainly is due to the less number of decision variables and constraints used in the proposed algorithm.

Other researchers based on a different approach in which a dynamic process model has been used have addressed the optimization of the TE process [3,4,10]. Most of these approaches and methods have also led to the production cost higher than 114 \$/h and those which resulted in the 114 \$/h are more computationally intensive comparing to the proposed method.

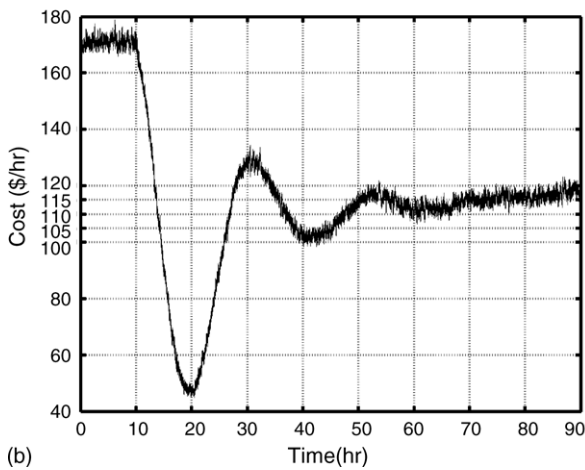
In order to study the optimality of the obtained result, some of the decision variables are perturbed around their optimum values. Fig. 7 shows the variation of cost function throughout the transient period caused by a slight change in mole percent of component 'B' in purge stream both in negative (−1.8%) and positive (0.5%) directions. The results corresponding to these changes are shown as test 1a and 1b in Table 4, respectively. The interesting point is the fact that despite a sharp decrease in the production cost, it gets to steady state value higher than the optimum production cost. In another study (test 2 in Table 4) the reactor pressure has been slightly changed from its optimum value (about 2800 kPa) to a lower value (2785 kPa), the effect of this change on production cost is shown in Fig. 8. The production cost at the steady state corresponding to this case is also higher (117 \$/h) than the optimum production cost.

The results of perturbing these two decision variables around their optimum values have also been shown in Table 4.





(a)



(b)

Fig. 7. Cost function in the case of changing the value of mole percent B in purge flow from its calculated value in both directions.

Perturbing the other decision variables around their optimum values would also lead to higher production cost at the steady state. This shows the optimality of the obtained operating conditions.

Figs. 9 and 10 show the change of product rate and its composition during the optimization. According to these fig-

Table 4  
Comparison of the objective function in the complementary test for optimization

Decision variable	Optimal values	Test 1a	Test 1b	Test 2
Reactor level (%)	65	65	65	65
Stripper level (%)	50	50	50	50
Separator level (%)	51.9	51.9	51.9	51.9
Product flow (cm/h)	22.949	22.949	22.949	22.949
Reactor Pressure (kPa)	2799.9	2799.9	2799.9	2785
Reactor Temperature (°C)	123.3	123.3	123.3	123.3
Compressor work (kW)	277	277	277	277
B in purge flow (%)	21.8	20	22.3	21.8
Recycle flow (kscmh)	32.2	32.2	32.2	32.2
E in product (%)	0.56	0.56	0.56	0.56
Cost function	114.2	118.1	116.2	117.2

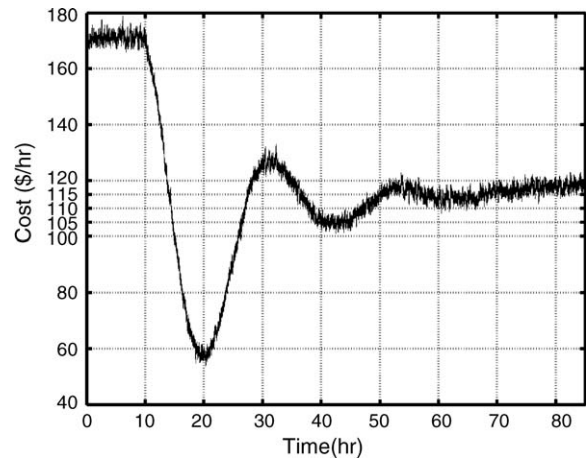


Fig. 8. Cost function in the case of changing the value of reactor pressure from its calculated value.

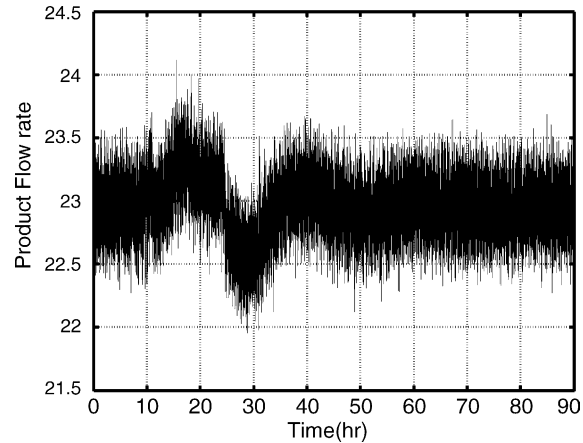


Fig. 9. Product flow rate variations during RTO.

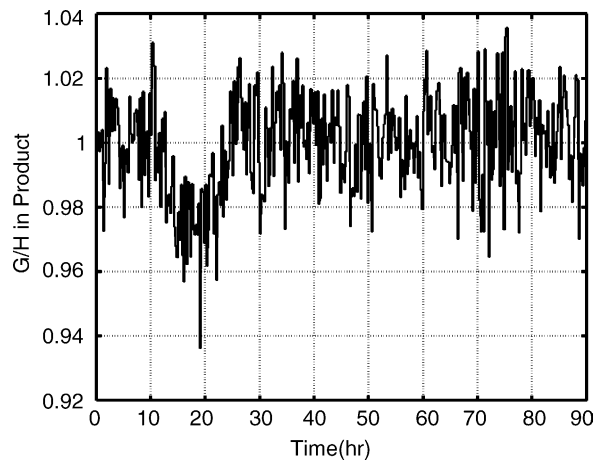


Fig. 10. G/H ratio variations during RTO.

ures the variations of product rate and composition remain in the limits defined by Dows and Vogel [5].

### 5.2. Alternative RTO scenario

The alternative optimization scenario that has been studied on the TE process for the base case roots in the fact that in most of the processes the product flow rate can change slightly around its nominal value. This is the case when the plant contains a product inventory which can fulfill market demands. In this case, the equality constraint corresponding to fixed production rate can be removed from the list of optimization constraints. Implementation of this scenario for the base case operation of the TE process leads to a solution with maximum product flow rate. However, this operating point is far from the base case and does not seem to be valid for the base case.

In order to keep the optimum point around the base case and yet avoiding the fixed product flow constraint, one can use an equality constraint corresponding to material balance around the stripper either for ‘G’ or ‘H’ Component. Using the material balance of ‘G’ around the stripper as an additional equality constraint and solving the optimization algorithm via the same algorithm would lead to a very interesting result. The optimization results in a point at which all the decision variables are near their corresponding values obtained previously except the production rate whose value is  $21.4 \text{ m}^3/\text{h}$ . This value for the production rate decreases the cost function by  $11.3 \text{ \$/h}$ . This cost reduction consists of two parts. The first part corresponds to the reduction of the product flow rate which is about  $1.57 \text{ \$/h}$ , whereas the second part which has the significant role in cost reduction corresponds to the change of operating conditions. Hence, the value of the objective function for this optimum point is about  $103 \text{ \$/h}$ . This means that the alternative optimization scenario presented in this section results in an extra saving which is about 10% of the original value. Table 5 and Fig. 11 show the value of decision variables at the optimum point and the trend of objective function through out the optimization, respectively.

Table 5  
Optimization near the base case condition

Decision variable	Base case value	Ricker's results	This paper results
Reactor level (%)	75	65	65
Stripper level (%)	50	50	50
Separator level (%)	50	50	51.9
Product flow (cm/h)	22.949	22.89	21.4
Reactor Pressure (kPa)	2705	2800	2799.7
Reactor Temperature (°C)	120.4	122.9	123.3
Compressor work (kW)	341.43	278.9	277
B in purge flow (%)	13.823	21.83	21.8
Recycle flow (kscmh)	26.902	32.18	32.2
E in product (%)	0.83570	0.58	0.56
Cost function	170.6	114.31	103.1

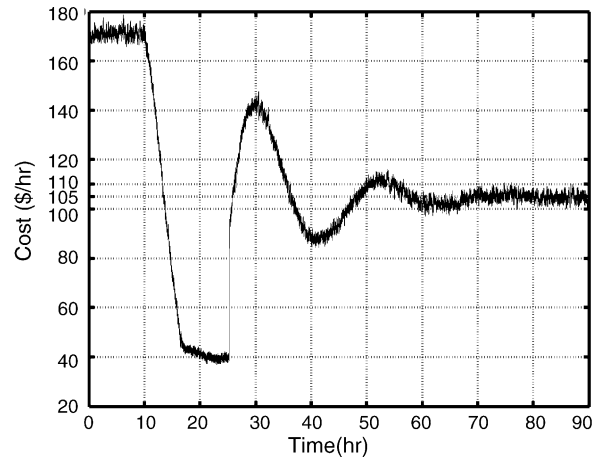


Fig. 11. Cost function at optimal operation condition near the base case.

## 6. Conclusions

This study has shown that the real time optimization of the TE plant can lead to operating condition at which the products can be obtained at a lower cost. It is shown by simulation that if correct decision variables and an enhanced optimization algorithm are chosen, the operating cost can be reduced by 33% which is a significant cost reduction. The optimum values obtained in this study are close to those reported by Ricker. However, these values have been obtained through on-line optimization and based on measurements corrupted by noise. The proposed method outperforms Riggs' method both in computational demand and optimization result. Riggs' formulation of RTO contained twice the number of variables as was used in the present study and their approach resulted in a considerably higher cost function than what obtained in this study.

It was also shown that with a small reduction in the production rate, RTO can provide an 8% improvement over the optimum cost function obtained for the original scenario at which the production rate was fixed at its base case value.

## Appendix A. TE process model

The model proposed by the Ricker for TE plant consists of differential equations corresponding to unsteady state material balance of various components for selected pieces of equipment:

$$\frac{dN_{i,r}}{dt} = y_{i,6}F_6 - y_{i,7}F_7 + \sum_{j=1}^3 v_{ij}R_j, \quad i = A, B, \dots, H \quad (\text{A.1})$$

$$\frac{dN_{i,s}}{dt} = y_{i,7}F_7 - y_{i,8}(F_8 + F_9) - x_{i,10}F_{10}, \quad i = A, B, \dots, H \quad (\text{A.2})$$

$$\frac{dN_{i,m}}{dt} = Z_{i,1}F_1 - Z_{i,2}F_2 + Z_{i,3}F_3 + y_{i,5}F_5 + y_{i,8}F_8 + F_i^* - y_{i,6}F_6, \quad i = A, B, \dots, H \quad (\text{A.3})$$

$$\frac{dN_{i,p}}{dt} = (1 - \phi_i)x_{i,10}F_{10} - x_{i,11}F_{11}, \quad i = G, H \quad (\text{A.4})$$

The above differential equations represent the internal states of the process model. These states are mapped into outputs (or measured variables) according to the following algebraic equations:

$$P_r = \sum_{i=A}^H P_{i,r}, \quad \begin{cases} P_{i,r} = \frac{N_{i,r}RT_r}{V_{Vr}}, & i = A, B, C \\ P_{i,r} = \gamma_{ir}x_{ir}P_i^{\text{sat}(T_r)}, & i = D, E, \dots, H \end{cases} \quad (\text{A.5})$$

$$V_{Vr} = V_r - V_{Lr}, \quad V_{Lr} = \sum_{i=D}^H \frac{N_{i,r}}{\rho_{i,r}} \quad (\text{A.6})$$

$$P_s = \sum_{i=A}^H P_{i,s}, \quad \begin{cases} P_{i,s} = \frac{N_{i,s}RT_s}{V_{Vs}}, & i = A, B, C \\ P_{i,s} = \gamma_{is}x_{i10}P_i^{\text{sat}(T_s)}, & i = D, E, \dots, H \end{cases} \quad (\text{A.7})$$

$$V_{Vs} = V_s - V_{Ls}, \quad V_{Ls} = \sum_{i=D}^H \frac{N_{i,s}}{\rho_{i,s}} \quad (\text{A.8})$$

$$F_6 = \pm\beta_6 \frac{2413.7}{M_6} \sqrt{|P_m - P_r|} \quad (\text{A.9})$$

$$P_m = \sum_{i=A}^H N_{i,m} \frac{RT_m}{V_m} \quad (\text{A.10})$$

$$F_7 = \pm\beta_7 \frac{5722.20}{M_7} \sqrt{|P_r - P_s|} \quad (\text{A.11})$$

$$F_{10} = F_{10}^P - F_{10}^* \quad (\text{A.12})$$

$$V_{Lp} = \frac{N_{G,p}}{\rho_G} + \frac{N_{H,p}}{\rho_H} \quad (\text{A.13})$$

$$y_{i,6} = \frac{N_{i,m}}{\sum_{i=A}^H N_{i,m}}, \quad i = A, B, \dots, H \quad (\text{A.14})$$

$$y_{i,8} = y_{i,9} = \frac{P_{i,s}}{P_s}, \quad i = A, B, \dots, H \quad (\text{A.15})$$

$$x_{i,11} = X_{GH} \frac{N_{i,p}}{N_{G,p} + N_{H,p}}, \quad i = G, H \quad (\text{A.16})$$

$$x_{i,r} = \begin{cases} 0, & i = A, B, C \\ \frac{N_{i,r}}{\sum_{i=D}^H N_{i,r}}, & i = D, E, \dots, H \end{cases} \quad (\text{A.17})$$

$$y_{i,7} = \frac{P_{i,r}}{P_r}, \quad i = A, B, \dots, H \quad (\text{A.18})$$

$$x_{i,10} = \begin{cases} 0, & i = A, B, C \\ \frac{N_{i,s}}{\sum_{i=D}^H N_{i,s}}, & i = D, E, \dots, H \end{cases} \quad (\text{A.19})$$

$$y_{i,5} F_5 = \begin{cases} Z_{i,4}F_4, & i = A, B, C \\ x_{i,10}F_{10}, & i = D, E, F \\ \phi_i x_{i,10}F_{10}, & i = G, H, (\phi_G = 0.07, \phi_H = 0.04) \end{cases} \quad (\text{A.20})$$

$$R_1 = \alpha_1 V_{Vr} \exp \left[ 44.06 - \frac{42600}{RT_r} \right] P_{A,r}^{1.08} P_{C,r}^{0.311} P_{D,r}^{0.874} \quad (\text{A.21})$$

$$R_2 = \alpha_2 V_{Vr} \exp \left[ 10.27 - \frac{19500}{RT_r} \right] P_{A,r}^{1.15} P_{C,r}^{0.370} P_{E,r}^{1.00} \quad (\text{A.22})$$

$$R_3 = \alpha_3 V_{Vr} \exp \left[ 59.50 - \frac{59500}{RT_r} \right] P_{A,r} (0.77 P_{D,r} + P_{E,r}) \quad (\text{A.23})$$

The above model consists of 26 internal states, 23 outputs, and 26 parameters. There is only 15 independent parameters among the total 26 parameters exist in the model. Ricker described the procedure through which the remaining 11 parameters can be obtained based on the independent ones. Tables A.1 and A.2 show the outputs and the independent parameters of the above model.

Table A.1  
Outputs of the process model

Model output number	Description
1	Reactor pressure (gage)
2	Reactor liquid level
3	Separator pressure (gage)
4	Separator liquid level
5	Stripper bottoms level
6	Stripper pressure (gage)
7	Reactor feed flow rate
8	A in reactor feed (stream 6)
9	B in reactor feed
10	C in reactor feed
11	D in reactor feed
12	E in reactor feed
13	F in reactor feed
14	A in purge (stream 9)

Table A.1 (Continued)

Model output number	Description
15	B in purge
16	C in purge
17	D in purge
18	E in purge
19	F in purge
20	G in purge
21	H in purge
22	G in product (stream 11)
23	H in product

Table A.2

Independent parameters of the model adjusted in the EKF

Parameter number	Symbol
1	100Z <sub>A4</sub>
2	100Z <sub>B4</sub>
3	100 $\alpha_1$
4	100 $\alpha_2$
5	F <sub>10</sub> *
6	100 $\beta_7$
7	100 $\beta_6$
8	100 $\chi_{GH}$
9	100 $\gamma_{GS}$
10	100 $\gamma_{HS}$
11	F <sub>C</sub> *
12	F <sub>D</sub> *
13	F <sub>E</sub> *
14	F <sub>F</sub> *
15	100 $\gamma_r$

## References

- [1] P.M. Duvall, J.B. Riggs, On-line optimization of the Tennessee Eastman challenge problem, *J. Process Control* 10 (2000) 19–33.
- [2] J.F. Forbes, T.E. Marlin, Design cost: a systematic approach to technology selection for model based real-time optimization, *Comp. Chem. Eng.* 20 (1996) 717–734.
- [3] T. Larson, K. Hestetun, E. Hovland, S. Skogestad, Self optimizing control of a large scale plant: the Tennessee Eastman process, *Ind. Eng. Chem. Res.* 40 (2001) 4889–4901.
- [4] T. Jokenhovel, L.T. Biegler, A. Wachter, Dynamic optimization of the Tennessee Eastman process using OptControlCentre, *Comp. Chem. Eng.* 27 (2003) 1513–1531.
- [5] J.J. Downs, E.F. Vogel, A plant-wide industrial process control problem, *Comp. Chem. Eng.* 17 (1993) 245–255.
- [6] N.L. Ricker, Optimal steady state operation of the Tennessee Eastman challenge process, *Comp. Chem. Eng.* 19 (1995) 949–989.
- [7] T.J. McAvoy, N. ye, Base control for the Tennessee Eastman problem, *Comp. Chem. Eng.* 18 (1994) 383–413.
- [8] N.L. Ricker, J.H. Lee, Nonlinear modeling and state estimation for the Tennessee Eastman challenge process, *Comp. Chem. Eng.* 19 (1995) 983–1005.
- [9] A. Gelb, J. Kasper, R.A. Nash, C.F. Price, A.A. Sutherland, *Applied Optimal Estimation*, The M.I.T. Press, 1974.
- [10] J.H. Lee, N.L. Ricker, Extended Kalman filter based non-linear model predictive control, *Ind. Eng. Chem. Res.* 33 (1994) 1530–1541.
- [11] N.L. Ricker, Decentralized control of the Tennessee Eastman challenge process, *J. Process Control* 6 (1996) 205–221.
- [12] A. Mirjalili, Application of artificial intelligence in real-time optimization of chemical processes, Master thesis, Department of Chemical and Petroleum Engineering, Sharif University of Technology, Tehran, Iran, 2001.
- [13] M.M. Javari, Plant-wide non-linear control of a chemical process, Master thesis, Department of Chemical and Petroleum Engineering, Sharif University of Technology, Tehran, Iran, 1999.